Design, Development and Experimental Investigation of H-rotor Vertical Axis Wind Turbine under Low Wind Speeds

Suhaib Mohammed*‡, Raghuram L Naik**

*Department of Electrical and Electronics Engineering, SECAB Institute of Engineering and Technology, Vijayapura-586 101, Karnataka, India.

**Department of Electrical and Electronics Engineering, Basaveshwar Engineering College, Bagalkot- 587 103, Karnataka, India.

(mohammed.pse1@gmail.com, naikrup1774@gmail.com)

‡Corresponding Author; Suhaib Mohammed, Department of Electrical and Electronics Engineering, SECAB Institute of Engineering and Technology, Vijayapura-586 101, Karnataka, India, Tel: +91 888 489 7759,

Fax: +91 835 227 7353, mohammed.pse1@gmail.com

Received: 21.03.2022 Accepted: 20.04.2022

Abstract- H-rotor vertical axis wind turbines (VAWT) are prominent wind energy converters for low wind speed applications due to their simple blade profile and efficient operation under turbulent wind conditions. This paper focuses on the design and development of H-rotor VAWT and its performance evaluation under low wind speeds. H-rotor VAWT is modelled in CATIA-v5 software with predetermined parameters such as blade profile, blade span, blade chord and turbine diameter for 25 W output power. Turbine blades are fabricated using low-cost and light-weight aluminium sheets and the H-rotor VAWT is developed using simple in-house fabrication techniques. A controlled wind environment with a wind speed range of 2.5 to 6.5 m/s is created using industrial fan blowers regulated by an autotransformer. The performance of the prototype is evaluated in terms of tip speed ratio (λ), output power (P), output torque (T) and C_p by varying the number of blades from two to five. The effect of solidity (quantified by variation in the number of blades) on the performance of the H-rotor VAWT is evaluated using different turbine characteristics. Reduced cut-in speed, high starting torque, increase in optimum λ and C_p are recorded for higher turbine solidity and an increase in the number of blades. However, this is attained at the expense of reduced peak power output for H-rotor models with a number of blades greater than three. The work presented in this paper would help researchers to design, develop, and perform experimental investigation and standardization of H-rotor VAWT for low wind speed operations.

Keywords- H-rotor, vertical axis wind turbine, design, development, performance analysis, low wind speed.

1. Introduction

Global electrical energy consumption is increasing rapidly and is expected to increase 90% of the current world electricity demand by the year 2040 [1]. In the past few decades, wind energy has emerged as one of the promising sources of energy to meet future electricity demands. In the year 2015, wind power generation amounts to be half of the global electricity growth [2]. However, it was estimated that the potential of wind energy can supply up to 40 times the world electricity demand. In this connection, large horizontal axis wind turbines (HAWTs) are contributing significantly to bridge the gap between current and estimated wind power generation. However, the large wind turbines have limitations in harvesting the geographically distributed wind energy present in the built environment due to the requirement of large space, a threat to human life and adverse climatic effects [3-5]. Small wind turbines (SWTs) with a typical power capacity of 1-10 kW are becoming popular for such deployments [6]. However, SWTs face the problem of poor performance in the built environment due to low speed and highly turbulent wind conditions. Further, high initial cost and effective placement are the major barriers to the dissemination of SWTs [7-8].

In recent decades, small HAWT systems have gained importance and commercialized for low wind speed applications, but, faced local resistance due to aesthetics, noise and various safety concerns [9]. Vertical axis wind turbines (VAWTs) are becoming a promising alternative to traditional HAWTs due to their low cost and ability to collect wind from all directions [6, 10]. The omnidirectional feature enables VAWT to operate efficiently under low speed and skewed wind conditions. It requires small space for its operation, produces less noise and offers more efficiency as compared to traditional HAWT. Further, the placement of the generator on the ground and small tower sway make the installation and maintenance much easier. H-rotor (Straight-bladed) turbine is found to be one of the popular VAWT systems due to ease in fabrication as it has a simple and symmetrical blade profile throughout the blade span [11-12]. However, these turbines are found to suffer from poor self-starting capability and low starting torque under low wind speed conditions.

Recent studies have revealed that turbine solidity (ratio of the area of the blades to rotor swept area) has a significant impact on starting characteristics of H-rotor VAWT such as cut-in speed, starting toque and self-starting capability. For H-rotor VAWT, turbine solidity (σ) is a function of the number of blades (N), blade chord (c) and turbine radius (R), as in Eq. (1).

$$\sigma = \frac{Nc}{R} \qquad (1)$$

High rotor solidity was found to yield better self-starting performance and higher power coefficients (C_p) at lower wind speeds. Improved self-starting capability, higher starting torque and C_p are recorded with higher values of σ achieved by increasing c and decreasing R [13-15]. Further, improved starting characteristics were observed with an increase in N yielding higher σ. However, the effect of σ quantified by variation in N is found to be uncertain on C_p and the overall performance of the H-rotor VAWT [16-18]. Further, studies conducted to analyse the effect of N on C_p have drawn mixed conclusions in this regard [19-23]. Further, it is found that standard design equations and testing procedures for small HAWTs have been developed by IEC (International Electrotechnical Commission), whereas, it has not been evolved for small VAWTs such as H-rotor due to lack of experimental data [24-25].

This paper aims to present detailed information for the design, development and experimental investigation of H-rotor VAWT under a low wind speed environment. Determination of the geometrical parameters, selection of blade profile and generator are described for the development of small H-rotor VAWT for the desired output power. The experimental setup, measurement system and methodology for the determination of important performance indicators of the wind turbine such as tip speed ratio (λ), output power (P), output torque (T) and C_p are presented in detail. The effect of σ quantified by variation in N on the performance of H-rotor VAWT is investigated through different turbine characteristics and validated against the qualitative results reported previously.

2. Design Parameters

2.1 Blade Span (l) and Turbine Diameter (d)

The H-rotor VAWT forms a cylinder with a rectangular cross-sectional area of width equal to blade span (l) and length equal to the diameter of the turbine (d) as shown in Fig 1.

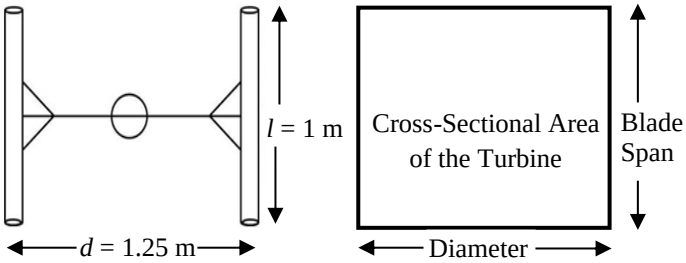

Fig 1: Cross-sectional View of H-rotor VAWT.

l and d are computed using power equation, as in Eq. (2),

$$P = \frac{1}{2} C_p \rho A v^3 \qquad (2)$$

Where,

P = Electrical output power of the turbine in W.

C_p = Power coefficient = 0.43 for H-rotor VAWT for maximum power production [26].

ρ = Air density = 1.173 Kg/m^3 (As determined in section 4.2)

A = Area of the cross-section of the turbine = $d * l$

v = Wind speed = 4.54 m/s (Average wind speed at the roof top of Vijayapura, India)

For 25 W output power, for generator efficiency of 85%, P is estimated as,

$$P = \frac{25}{85} * 100 = 29.41 \text{ W}$$

For small Darrious VAWT such as H-rotor, l = 1 m is assumed [27] and d is obtained using Eq. (2) as 1.246 ≈ 1.25 m.

2.2. Blade Chord (c)

Chord length (c) of the blade is the length of the imaginary line joining the leading and trailing edges of an aerofoil as shown in Fig 2.

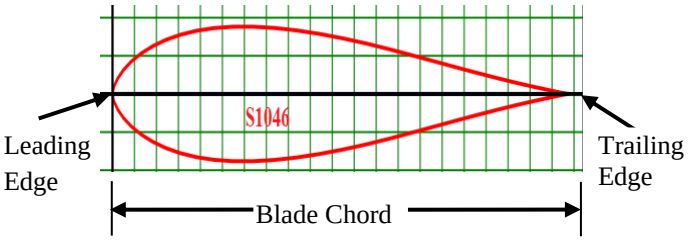

Fig 2. Cross-section of S-1046 aerofoil.

c is obtained, as in Eq. 3,

$$\text{Aspect Ratio} = (AR) = \frac{l}{c} \qquad (3)$$

The optimal AR for H-rotor VAWT is reported to be in the range of $10 < AR < 20$ [28]. Considering an aspect ratio of 10,

a blade chord of 0.1 m is obtained for the blade span of 1 m using Eq. (3).

2.3. Number of Blades (N) and Turbine Solidity (σ)

In the present work, the number of blades (N) are varied from two to five and the corresponding turbine solidity (σ) is determined by using Eq. (1), keeping c and R constant as shown in Table 1. The top view of H-rotor VAWT models with N = 2, 3, 4 and 5 are shown in Fig 3.

Table 1. Turbine Solidity for N = 2, 3, 4 and 5.

Number of Blades (N)	Chord (c) in m	Radius (R = $d/2$) in m	Turbine Solidity (σ)
2	0.1	0.625	0.32
3	0.1	0.625	0.48
4	0.1	0.625	0.64
5	0.1	0.625	0.8

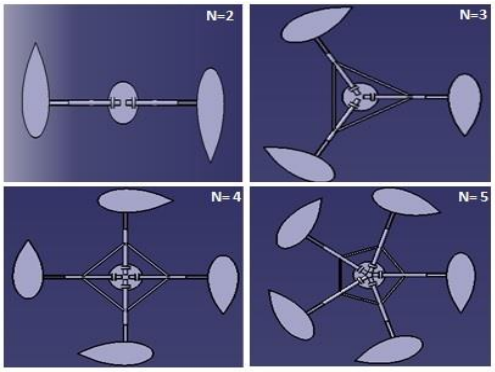

Fig 3. Top view of H-rotor VAWT for N = 2, 3, 4 and 5.

2.4. Blade Aerofoil

The commonly used aerofoils for H-rotor VAWT are NACA00xx series [29-31]. However, recently S series aerofoils, predominantly the S-1046 blade profile is proposed as the optimal configuration for H-rotor VAWT. The performance characteristics of the standard NACA and S series aerofoils in terms of the C_p- λ curves are shown in Fig 4 (a) and (b) respectively [32]. A maximum C_p of 0.4051 was recorded for the S-1046 profile with a relative increase of 26.83% as compared to standard NACA aerofoils. Therefore, the S-1046 profile is preferred for the development of turbine blades. Symmetrical aerofoil is kept along the blade span to obtain symmetrical lift and drag forces on the upper and lower portions of the blade. This characteristic of aerofoil provides lift during the 360° operation of the turbine.

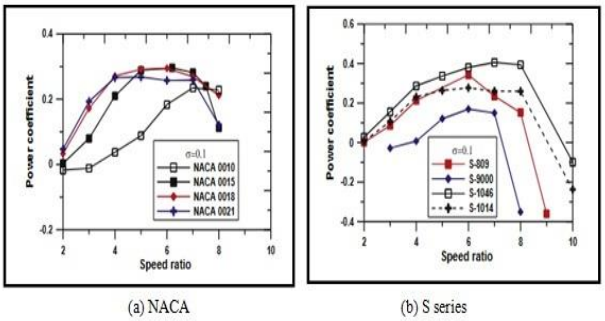

(a) NACA (b) S series

Fig 4. Performance of H-rotor VAWT for NACA and S series aerofoils [32].

2.5. Generator

Direct–drive wind generators are most promising for SWT applications due to higher overall efficiency, reliability and gearless operation [32]. Recently, direct-drive permanent magnet synchronous generators (PMSG) have become economically viable for SWTs due to the improved performance and reduced cost of permanent magnetic materials [33-37]. In the present work, to obtain 25 W output power, 50 W PMSG is used to avoid the electric breakdown in case of excess power during gusty wind conditions. The nominal properties of PMSG are given in Table 2.

Table 2. Nominal properties of PMSG

Type	Salient pole single phase PMSG
Power (W)	50
Voltage (V)	24
Current (A)	2.5
Efficiency	85%
Rotational Speed (RPM)	70
Number of poles	4
Height (m)	0.07
Diameter (m)	0.17
Weight (Kg)	3.59

3. Fabrication of H-rotor VAWT

The CATIA v5 software is used to develop 3D models of H-rotor VAWT for N = 2, 3, 4 and 5 using predetermined parameters as described in section 2. The 3D model of the five-blade H-rotor VAWT is shown in Fig 5.

H-rotor blades of S-1046 aerofoil are fabricated using aluminium sheets as shown in Fig 6. An iron bar (a1) of 750 mm * 55 mm * 2 mm is bolted at the middle of each blade such that the vertical edges of the bar are placed at the distance of 135 mm and 60 mm from the trailing and leading edges of the blade along the chord length respectively. Iron strut (a1) of

500 mm * 10 mm * 10 mm is welded to each iron bar (a1) at the middle and connected to the circular iron hub having a diameter of 200 mm and thickness of 7 mm. To provide solidity to the turbine, an iron strut (a2) of 260 mm * 10 mm * 10 mm is connected between the iron struts (a1) at a

distance of 220 mm from the centre of the hub. To strengthen the linkage between struts and blade, an iron bar (a2) of 212 mm* 10 mm * 2 mm is welded between iron strut (a1) and iron bar (a1) on either side. A hollow iron cylinder of height 50 mm with an internal diameter of 10 mm and an external diameter of 15 mm is welded at the centre of the hub for directly coupling the turbine with the shaft of PMSG. The design parameters of the developed H-rotor VAWT are listed in Table 3.

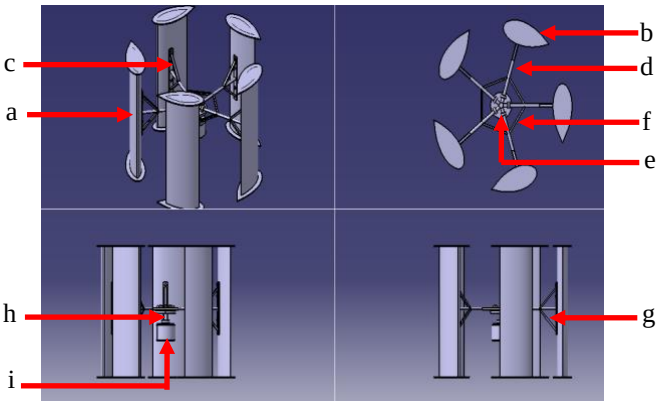

Fig 5. 3D model of five-blade H-rotor VAWT, **a.** Blade, **b.** Streamlined sheet, **c.** Iron bar (a1), **d.** Iron strut (a1), **e.** Iron hub, **f.** Iron strut (a2), **g.** Iron bar (a2), **h.** Hollow iron cylinder, **i.** PMSG.

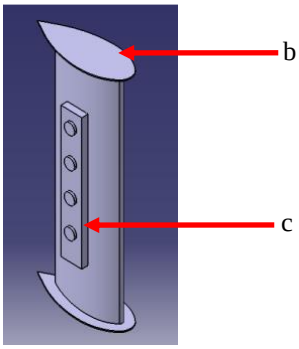

Fig 6. 3D model of H-rotor blade.

Table 3. Design parameters of the H-rotor VAWT

Turbine Type	H-rotor VAWT
Blade Aerofoil	S-1046
Blade material	Aluminium
Blade chord (m)	0.25
Blade span (m)	1
Turbine Diameter (m)	1.25
Swept Area (m^2)	1.25
Weight (Kg)	12.03

4. Experimental Details

4.1. Experimental Setup

The experimental setup of H-rotor VAWT consists of a wind chamber, wind speed control system, turbine mount assembly and measuring instruments. The 3D model of the setup is shown in Fig 7.

A. Wind Chamber

The experimental setup consists of a wind chamber of 2.5 m * 1.5 m * 1.5 m, which is closed from all the sides using transparent fibre sheets except the front and back sides. The chamber width can be adjusted from 0.5 m to 1.5 m to accommodate VAWTs of diameter ranging from 0.4 m to 1.4 m (keeping a 0.05 m gap from both sides of the chamber). An iron tube (b1) of 1.5 m * 10 mm * 10 mm is welded horizontally at the middle on the backside of the chamber. For the developed H-rotor VAWT of diameter 1.25 m, chamber width is adjusted to 1.35 m and two industrial fans are fixed on an iron tube (b1) such that the hub of each fan is placed at a distance of 0.425 m from either side of the wind chamber.

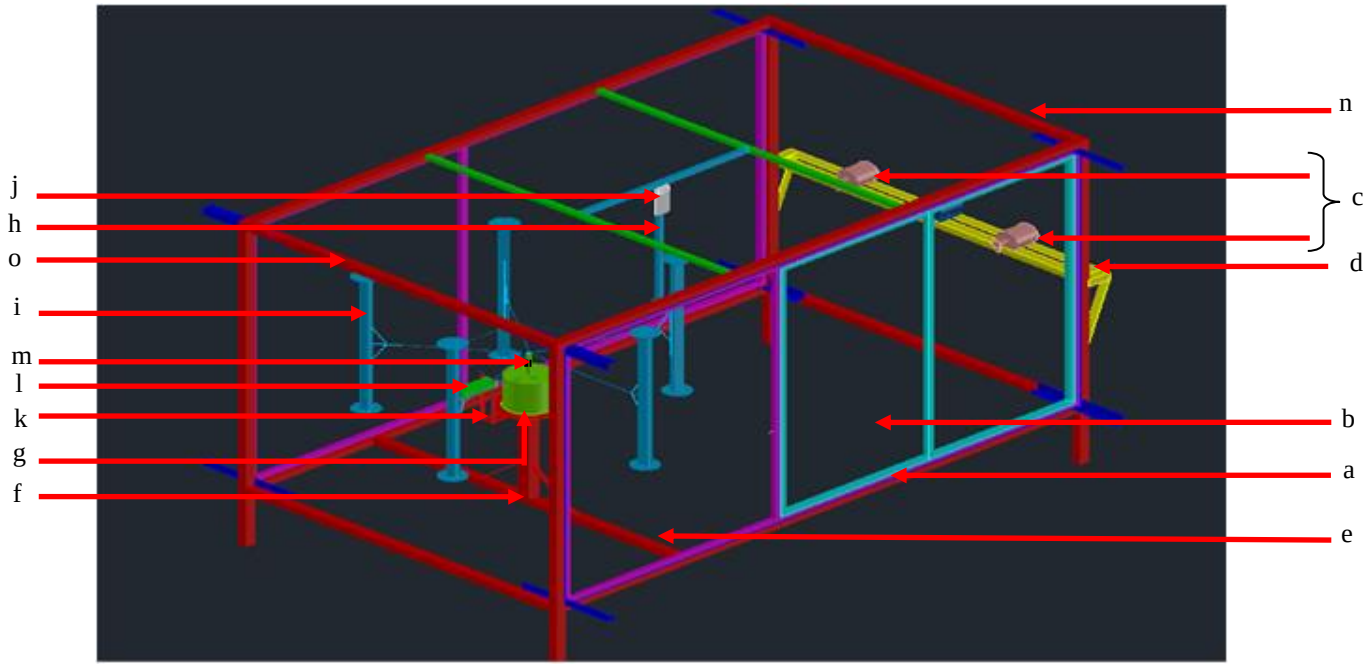

Fig.7. 3D model of the experimental setup, **a.** Wind chamber, **b.** Transparent fibre sheet, **c.** Industrial fans, **d.** Iron tube (b1), **e.** Iron tube (b2), **f.** Iron tube (b3), **g.** Circular iron plate, **h.** Iron tube (b4), **i.** H-rotor VAWT, **j.** Digital display of anemometer, **k.** Extended iron bar arrangement, **l.** Tachometer, **m.** Reflective piece, **n.** Backside, **o.** Front side.

B. Wind Speed Control System

Two industrial fans (230 V, 175 W) of diameter 0.6 m and a flow rate of 90 m^3/s are used to create the controlled wind environment. The armature voltage speed control method is employed to control the speed of fans to obtain a low wind speed range of 2.5 to 6.5 m/s. This is achieved by using a single-phase autotransformer (270 V, 10 A) connected in parallel with both the fans to maintain equal input voltages.

C. Turbine Mount Assembly

Iron tube (b2) of 1.5 m * 2.5 cm * 2.5 cm is welded at the bottom side of the wind chamber at a distance of 0.5 m from the front side of the chamber. An iron tube (b3) of 0.7 m * 5 cm * 5 cm supported by two iron tubes of 0.35 m * 2.5 cm * 2.5 cm is welded vertically at the middle of the iron tube (b2). The other side of the iron tube (b3) is welded to the centre of the circular iron plate having a diameter and thickness of 400 mm and 7 mm respectively. The PMSG is fixed on the circular iron plate and the developed H-rotor VAWT is then coupled with the shaft of the PMSG.

4.2 Data Logging System

The generator output terminals are connected to a 12 V battery through the rectifier, filter and 12 V regulator circuit as depicted in Fig 8. The autotransformer regulates the voltage applied to the industrial fan blowers to obtain desired wind speed in the wind chamber. Then H-rotor VAWT rotates and generates fluctuating A.C electrical output power. The rectifier converts fluctuating A.C into fluctuating D.C electrical power. The regulator circuit stabilizes the fluctuating D.C to 12 V constant D.C electrical power.

The measurement techniques adopted to obtain desired parameters are detailed as follows,

A. Wind Speed (v)

Wind speed (v) is measured by vane type anemometer (BEETECH AM-4208), which is placed such that an adequate distance is maintained between the turbine and anemometer during the experimentation, otherwise, the turbine may throw back the turbulent wind during its operation. For this purpose, an iron tube (b4) of 0.7 m * 5 cm * 5 cm is welded and dropped from the top of the wind chamber at a distance of 0.5 m from the outer periphery of the turbine. The digital display of the anemometer is fixed at the top and the spinning fan is fixed at the bottom of the iron tube (b4).

B. Air Density (ρ)

Air density (ρ) is determined, as in Eq. (4),

$$\rho = \frac{P_{av}}{R*T} \quad (4)$$

Where,

P_{av} = Average air pressure measured using weather forecaster (Xcluma digital compass) = 100500 pa (1005 mb).

R = Specific gas constant for dry air = 287.05 J.

T = Average temperature measured using weather forecaster (Xcluma digital compass) = 298.35 K (25.2^0).

From the above data, ρ is obtained as 1.173 Kg/m^2 using Eq. (4).

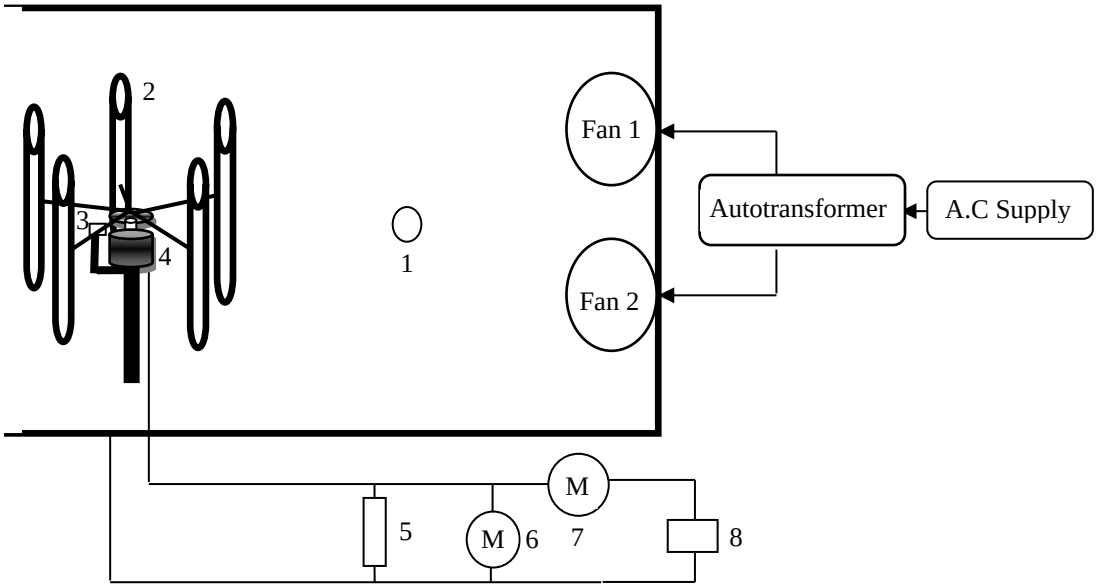

Fig 8. Schematic of the experimental setup, **1.** Anemometer, **2.** H-rotor VAWT, **3.** Tachometer, **4.** PMSG, **5.** Rectifier and filter circuit, **6.** Multimeter for voltage measurement, **7**. Multimeter for current measurement, **8.** Battery.

C. Turbine speed (n)

For measuring turbine speed (*n*), an infrared (IR) sensor-based tachometer is used, which is fixed on an extended iron bar welded to the turbine mount assembly such that the IR light is pointed at the reflective piece of black adhesive tape pasted on the generator shaft as depicted in Fig 7. An optimum and constant light environment is maintained during the conduction of the experiments to avoid the distraction of the IR light.

D. Output voltage (V_{dc}) and current (I_{dc})

The output voltage (V_{dc}) and output current (I_{dc}) are measured using two multimeters (HTC-DM-97) connected in parallel and series between the rectifier circuit and battery respectively as shown in Fig 8.

E. Power coefficient (C_p)

Power coefficient (C_p) is a measure of aerodynamic efficiency of the turbine and it is obtained, as in Eq. (5).

$$C_p = \frac{P_e}{(0.5\rho A v^3)} \tag{5}$$

The mean electric output power (P_e) of the turbine at a particular wind speed is calculated, as in Eq. (6),

$$P_e = \frac{1}{m}\sum_{i=1}^{m} V_{dc,i} * I_{dc,i} \tag{6}$$

Where, *m* is the number of observations made at a particular wind speed, $V_{dc,i}$ and $I_{dc,i}$ are rectified output voltage and current for ith observation respectively.

Using Eq. (5) and Eq. (6), C_p at a particular wind speed is calculated, as in Eq. (7),

$$C_p = \frac{P_e}{(0.5\rho A v^3)} \tag{7}$$

F. Tip speed ratio (λ)

The tip speed ratio (λ) is given, as in Eq. (8),

$$\lambda = \frac{\text{Tip speed of the blade}}{\text{Wind Speed}} = \frac{\omega * R}{v} \tag{8}$$

Where, ω is the angular speed of the turbine in rad/s, *R* is the radius of the turbine in m and *v* is the wind speed in m/s. Mean λ at a particular wind speed is given, as in Eq. (9),

$$\omega_i = \frac{2*\pi*n_i}{60} \tag{9}$$

Where, ω_i is the angular speed of the turbine in rad/s for ith observation at a particular wind speed and is given, as in Eq. (10),

$$\omega_i = \frac{2*\pi*n_i}{60} \tag{10}$$

Where, n_i is turbine speed in rpm for ith observation at a particular wind speed.

G. Turbine torque (T)

Turbine torque (*T*) determines the force acting on the turbine about its axis. The output power of any rotating body is given, as in Eq. (11),

$$P = T * \omega \tag{11}$$

Using Eq. (12), the mean torque developed by the turbine at a particular wind speed is calculated as,

$$T = \frac{1}{m}\sum_{m=1}^{i} \frac{P_e}{\omega_i} \tag{12}$$

5. Results and Discussion

The performance analysis of the developed H-rotor VAWT is carried out under a low wind speed environment created by the experimental setup described in section 4.1. The various parameters as described in section 4.2 are determined by varying the number of blades from two to five. The measurements are performed for three observations (m = 3) at particular wind speeds. Sample measurements for the five-blade H-rotor model are presented in Table 4.

Table 4. Computation of various parameters for five-blade H-rotor VAWT

Sl.No.	V	N	V_{dc}	I_{dc}	P	T	C_p	λ
1	**2.7**	9	**12.1**	0	0	0	**0**	0.217
		9		0	0	0		0.217
		9		0	0	0		0.217
		9		**0**	**0**	**0**		**0.217**
2	**2.8**	13	**12.1**	0.047	0.569	0.418	**0.036**	0.302
		12		0.046	0.557	0.443		0.279
		14		0.048	0.581	0.396		0.325
		13		**0.047**	**0.569**	**0.419**		**0.303**
3	**3.2**	21	**12.1**	0.315	3.812	1.4	**0.161**	0.427
		21		0.316	3.824	1.405		0.427
		22		0.32	3.872	1.37		0.447
		21.33		**0.317**	**3.836**	**1.691**		**0.434**
4	**3.4**	27	**12.1**	0.491	5.941	2.101	**0.208**	0.516
		27		0.493	5.965	2.11		0.516
		27		0.495	5.99	2.119		0.516
		27		**0.493**	**5.965**	**2.11**		**0.516**
5	**3.7**	30	**12.1**	0.8	9.68	3.081	**0.264**	0.527
		31		0.8	9.68	2.982		0.545
		31		0.812	9.825	3.027		0.545
		30.67		**0.804**	**9.728**	**3.03**		**0.539**
6	**4.2**	38	**12.1**	1.635	19.784	4.972	**0.367**	0.588
		37		1.628	19.699	5.084		0.573
		38		1.636	19.796	4.975		0.588
		37.67		**1.633**	**19.76**	**5.01**		**0.583**
6	**4.7**	43	**12.1**	2.199	26.608	5.909	**0.352**	0.595
		43		2.2	26.62	5.912		0.595
		42		2.195	26.56	6.039		0.581
		42.67		**2.198**	**26.596**	**5.953**		**0.59**
7	**5.2**	47	**12.1**	2.315	28.012	5.692	**0.274**	0.588
		47		2.316	28.024	5.694		0.588
		48		2.32	28.072	5.585		0.6
		47.33		**2.317**	**28.031**	**5.657**		**0.592**
8	**5.7**	52	**12.1**	2.239	27.092	4.976	**0.201**	0.592
		52		2.239	27.092	4.976		0.592
		53		2.242	27.128	4.888		0.604
		52.33		**2.24**	**27.104**	**4.947**		**0.596**
10	**6.2**	57	**12.1**	1.878	22.724	3.807	**0.131**	0.598
		58		1.89	22.869	3.765		0.608
		57		1.872	22.651	3.795		0.598
		57.33		**1.88**	**22.748**	**3.789**		**0.601**

The effect of solidity and the number of blades on the performance of the H-rotor VAWT is evaluated through different turbine characteristics as described below.

5.1. λ - v curve

The variation of tip speed ratio (λ) as a function of wind speed (v) is depicted in Fig 9. λ is a measure of the rotational speed of the turbine (n). High values of λ at lower wind speeds result in a higher rotational speed of the turbine and yield better starting characteristics. In Fig 9, initial values of λ for two and three-blade H-rotor models are recorded at a wind speed of 3.2 m/s, which indicates that two and three-blade H-rotor models have started rotating at 3.2 m/s. Initial values of λ for four and five-blade H-rotor models are observed at a wind speed of 2.8 m/s and 2.7 m/s respectively, which indicates that four and five-blade H-rotor models have started rotating at a wind speed of 2.8 m/s and 2.7 m/s respectively. It can also be seen that four and five-blade H-rotor models have higher values of λ as compared to two and three-blade H-rotor models in a low wind speed range of 2.7 to 5.2 m/s. However, the five-blade H-rotor model has performed significantly well and obtained higher values of λ as compared to the four-blade H-rotor model. Stable values of λ are observed for four and five-blade H-rotor models between wind speed range of 4.7 to 6.2 m/s, which indicates that four and five-blade H-rotor models have attained constant turbine speed and reached their rated output power. For two and three-blade models, a small rise in values of λ between wind speed range of 5.2 to 5.7 m/s is observed, however, it is negligible.

From the above discussion, it is clear that reduced cut-in speed and higher values of λ resulting in higher turbine speed are obtained with an increase in the number of blades i.e. at higher solidity. Therefore, the present work justifies the work presented in [18, 23], where, λ and turbine speed of H-rotor VAWT are reported to be enhanced for higher solidity and an increase in the number of blades.

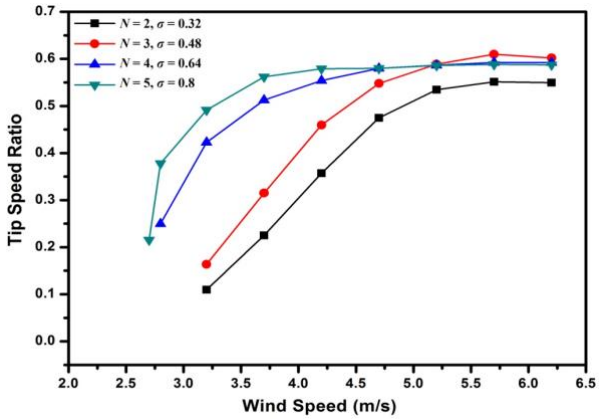

Fig 9. λ - v curve.

5.2. P_e - v curve

The power curve (P_e vs v) is plotted to determine the effect of solidity and number of blades on output power as shown in Fig 10. The various characterizations such as cut-in and cut-out speeds, rated output power and area under the curve (from cut-in to cut-out wind speed) for two, three, four and five-blade H-rotor models are presented in Table 5.

Table 5. Various characterizations of H-rotor VAWT models.

Number of blades	Solidity	Cut-in speed (m/s)	Cut-out speed (m/s)	Rated output power (Watt)	Area under the curve (m^2)
Two	0.32	3.7	5.7	22.208	57.00
Three	0.48	3.4	5.7	30.14	82.01
Four	0.64	3.2	5.2	25.144	60.97
Five	0.8	2.8	5.2	28.031	72.56

As can be seen from Fig 10, reduced cut-in speeds are obtained at higher solidity with the increase in the number of blades. Therefore, the power curves have shifted towards a low wind speed region with an increase in the number of blades. This is due to the high turbine torque developed by H-rotor VAWT due to an increase in drag forces acting on the turbine with an increase in the number of blades as depicted in Fig 11.

The three-blade H-rotor model has attained higher output torque as compared to other H-rotor models as it offers less turbulence to wind at higher turbine speeds. Whereas, H-rotor models with a higher number of blades (N>3) behave as a hollow cylinder and block the wind at higher turbine speeds. This has resulted in higher output power for three-blade H-rotor VAWT as compared to other H-rotor models.

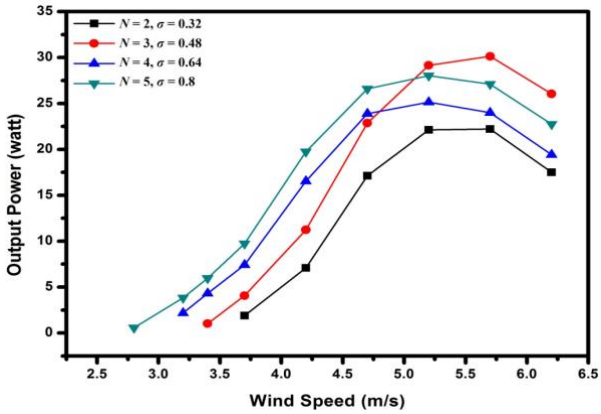

Fig 10. P_e - v curve.

5.3. C_p - λ Curve

The power coefficient curve (C_p *vs* λ) is plotted to determine the effect of solidity and number of blades on C_p as shown in Fig 12. The maximum C_p of 0.367 is obtained

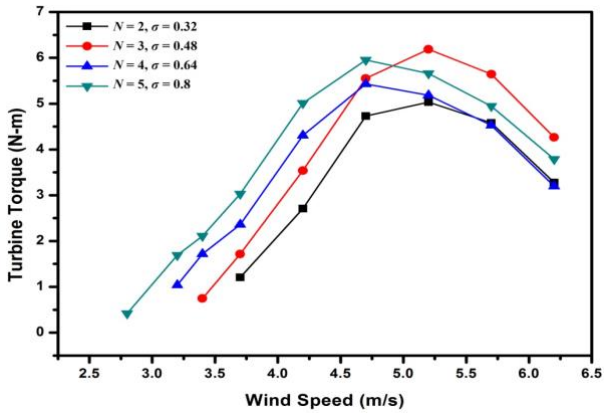

Fig 11. T- v curve.

for five-blade H-rotor models at λ= 0.583, whereas, four, three and two-blade H-rotor models have obtained a maximum C_p of 0.316, 0.303 and 0.227 at λ= 0.581, 0.544 and 0.479 respectively. These results revealed that optimum C_p and λ increase at higher solidity values with an increase in the number of blades. Therefore, the present work justifies the results presented in [19-20], that the peak of C_p increases with an increase in the number of blades, in contrast with results produced by Rezaeiha et al. [17], Maeda T et al. [18] and Abu-El-Yazid et al. [22], where, optimum C_p is reported to be unaffected or decreased at higher solidities with an increase in the number of blades. Further, optimum λ is found to be increased with an increase in the number of blades and thus, solidity as presented in [18], in contrast with the results presented in [20,22], where, optimum λ is reported to be decreased for higher solidity and increase in the number of blades.

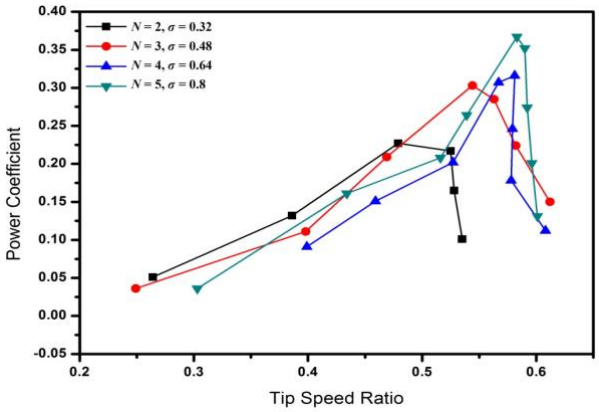

Fig 12. C_p - λ curve.

Conclusion

In this paper, the design and development of H-rotor VAWT are presented in detail. The development of an experimental setup and methodology for the performance analysis of H-rotor VAWT under low wind speeds is presented. The effect of solidity (quantified by variation in the number of blades) on the starting characteristics and overall performance of H-rotor VAWT is clarified

The following inferences are drawn from the experimental results,

- Improved starting characteristics such as higher tip speed ratios, low cut-in speed and high starting torque are recorded for higher solidity with an increase in the number of blades.
- The optimum tip speed ratio and power coefficient are observed to be increasing for higher solidity with an increase in the number of blades.
- The reduced peak output power and higher turbulence to wind are recorded for higher solidity with the number of blades greater than three.
- Higher output power, significantly better power curve and higher output torque are recorded for the three-blade H-rotor model.

In view of the above observations, this study concludes that starting characteristics and efficiency of the H-rotor VAWT can be enhanced for higher solidity with an increase in the number of blades. However, it can be achieved at the expense of reduced peak output torque and power. Therefore, the three-blade H-rotor model (with moderate power coefficient and solidity) is proposed as an optimal configuration for better overall performance under low wind speeds. This study would be helpful in the selection and computation of design parameters, development of experimental setup and performance analysis for future developments and standardization of H-rotor VAWT.

Acknowledgement

This work was supported by the Visveshvesvaraya Technological University (VTU), Belagavi, India under its TEQIP 1.3 competitive research grant vide VTU/TEQIP 3/2019/321.

References

[1] World energy outlook 2018, Available at: https://iea.blob.core.windows.net/assets/77ecf96c-5f4b-4d0d-9d93 d81b938217cb/World_Energy_Outlook_2018.pdf, accessed January 2023. (Report)

[2] Global wind statics 2015, Available at: https://www.gwec.net/wp-content/uploads/vip/GWEC-PRstats-2015_LR.pdf, accessed January 2023. (Report)

[3] W. Chien, and R. G. Prinn, "Potential climatic impacts and reliability of very large-scale wind farms", Atmos. Chem. Phys., DOI:10.5194/acp.2010.10.2053,Vol. 10, No. 4, pp. 2053-2061, February 2010. (Article)

[4] D. Kaoshan, A. Bergot, C. Liang, W. Xiang, and Z. Huang, "Environmental issues associated with wind energy–A review", Renewable Energy, DOI:10.1016/j.renene.2014.10.074, Vol. 75, pp. 911-921, March 2015. (Article)

[5] M. Premalatha, T. Abbasi, and S. A. Abbasi, "Wind energy: Increasing deployment, rising environmental concerns", Renewable and Sustainable Energy Rev., DOI:10.1016/j.rser.2013.11.019, Vol. 31, pp. 270-288, March 2014. . (Article)

[6] K. C. Anup, J. Whale, and T. Urmee, "Urban wind conditions and small wind turbines in the built environment: A review", Renewable energy, DOI:10.1016/j.renene.2018.07.050, Vol. 131, pp. 268-283, February 2019. (Article)

[7] W. T. Chong, A. Fazlizan, S. C. Poh, K. C. Pan, and H. W. Ping, "Early development of an innovative building integrated wind, solar and rain water harvester for urban high rise application", Energy Build., DOI:10.1016/j.enbuild.2011.11.041, Vol. 47, pp. 201-207, April 2012. (Article)

[8] D. Li, S. Wang and P. Yuan, "A review of micro wind turbines in the built environment", Asia-Pacific Conference on Power and Energy Engineering, China, pp. 1-4, 28-31 March 2010. (Conference paper)

[9] A. Noor, and M. Cameron, "The challenges and possible solutions of horizontal axis wind turbines as a clean energy solution for the future", Renewable and Sustainable Energy Rev., DOI:10.1016/j.rser.2014.06.004, Vol. 38, pp. 439-460, October 2014. (Article)

[10] M. M. A. Bhutta, N. Hayat, , A. U. Z. Farooq Ali, S. R., Jamil, and Z. Hussain, "Vertical axis wind turbine–A review of various configurations and design techniques", Renewable and Sustainable Energy Rev., DOI:10.1016/j.rser.2011.12.004, Vol. 4, No. 16, pp. 1926-1939, May 2012. (Article)

[11] A. Oguz, D. Syed, and S. Demirbas. "A Review of Wind Energy Conversion Systems." 10th International Conference on Smart Grid (icSmartGrid), IEEE, Istanbul, Turkey, pp. 72-77, 27-29 June 2022.

[12] M. Abdullah, A. Gasaymeh, M. Shalby, and H. Al-Rawashde, "Review of Effect of Specific Geometrical Parameters on the Performance of Small Straight Blade–Vertical Axis Wind turbine (SB-VAWTs) of Darrieus-type", Int. J. Renewable Energy Res., DOI: 10.20508/ijrer.v11i4.12420.g8343, Vol.11, No.4, December 2021. (Article)

13] Y. X. Peng, Y. X., Y. L. Xu, S. Zhan and K. M. Shum "High-solidity straight-bladed vertical axis wind turbine: Aerodynamic force measurements", J. Wind Eng. Ind. Aerodyn., DOI:10.1016/j.jweia.2018.11.005, Vol. 184, pp. 34-48, January 2019. (Article)

14] L. Du, G. Ingram, and R. G. Dominy, "Experimental study of the effects of turbine solidity, blade profile, pitch angle, surface roughness, and aspect ratio on the H-Darrieus wind turbine self-starting and overall performance", Energy Sci. Eng. , DOI:10.1002/ese3.430, Vol. 7, No. 6, pp. 2421-2436, August 2019. (Article)

15] M. F. Ramlee, A. Fazlizan and S. Mat, "Performance Evaluation of H-Type Darrieus Vertical Axis Wind Turbine with Different Turbine Solidity", J. Comput. Theor. Nanosci., DOI:10.1166/jctn.2020.8726, Vol. 17, No. 2-3, pp. 833-839, February 2020. (Article)

16] A. Sagharichi, M. Zamani and A. Ghasemi, "Effect of solidity on the performance of variable-pitch vertical axis wind turbine", Energy, DOI:10.1016/j.energy.2018.07.160, Vol.161, pp.753-775, October 2018. (Article)

17] Rezaeiha, Abdolrahim, H. Montazeri and B. Blocken, "Towards optimal aerodynamic design of vertical axis wind turbines: Impact of solidity and number of blades", Energy, DOI:10.1016/j.energy.2018.09.192, Vol. 165, pp. 1129-1148, December 2018. (Article)

18] T. Maeda, Y. Kamada, J. Murata, K. Shimizu, T. Ogasawara, A. Nakai and T. Kasuya, "Effect of solidity on aerodynamic forces around straight-bladed vertical axis wind turbine by wind tunnel experiments (depending on number of blades)", Renewable Energy, DOI:10.1016/j.energy.2018.09.192, Vol. 96, pp. 928-939, October 2016. (Article)

[19] M. El-Samanoud, A. A. E. Ghorab, and Sh. Z. Youssef, "Effect of some design parameters on the performance of a Giromill vertical axis wind turbine", Ain Shams Eng. J., DOI:10.1016/j.asej.2010.09.012, Vol. 1, No. 1, pp. 85-95. (Article)

[20] M. R Castelli, S. D. Betta, and E. Benini, "Effect of blade number on a straight-bladed vertical-axis Darreius wind turbine", World Academy Sci., Eng. Technol., DOI:10.5281/zenodo.1079974, Vol. 61, pp. 305-3011, January 2012. (Article)

[21] T. Maeda, Y. Kamada, J. Murata, K. Furukawa, and M. Yamamoto, "Effect of number of blades on aerodynamic forces on a straight-bladed Vertical Axis Wind Turbine", Energy, DOI:10.1016/j.energy.2015.07.115, Vol. 90, pp.784-795, October 2015. (Article)

[22] Abu-El-Yazied, G. Taher, M. A. Ahmad., M. S. Al-Ajmi, and I. M. Hassan, "Effect of number of blades and blade chord length on the performance of Darrieus wind turbine", Am. J. Mech. Eng. Autom., Vol. 2, No. 1, pp. 16-25, January 2015. (Article)

[23] Kavade, K. Ramesh, and M. P. Ghanegaonkar, "Design and analysis of vertical axis wind turbine for household application", J. of Clean Energy Technol., DOI: 10.18178/jocet.2017.5.5.39, Vol. 5, No. 5, pp. 353-358. September 2017. (Article)

[24] M. Abid, K. S. Karimov, H. A. Wajid, F. Farooq, H. Ahmed, and O. H. Khan, "Design, development and testing of a combined Savonius and Darrieus vertical axis wind turbine", Iran. J. Energy Environ., DOI:10.5829/idosi.ijee.2015.06.01.02, Vol. 6, No. 1, pp. 1-4. December 2014. (Article)

[25] Lee, Kung-Yen, Shao-Hua Tsao, Chieh-Wen Tzeng, and Huei-Jeng Lin, "Influence of the vertical wind and wind direction on the power output of a small vertical-axis wind turbine installed on the rooftop of a building", Appl. Energy, DOI:10.1016/j.apenergy.2017.08.185, Vol. 209, pp. 383-391, January 2018. (Article)

[26] Hameed, M. Saqib, and S. K. Afaq, "Design and analysis of a straight bladed vertical axis wind turbine blade using analytical and numerical techniques," Ocean Eng., DOI:10.1016/j.oceaneng.2012.09.007, Vol.57, pp.248-255, January 2013. (Article)

[27] G. Abdalrahman, W. Melek and F. S. Lien, "Pitch angle control for a small-scale Darrieus vertical axis wind turbine with straight blades (H-Type VAWT)", Renewable Energy, DOI:10.1016/j.renene.2017.07.068, Vol. 114, pp. 1353-1362, December 2017. (Article)

[28] M. Ahmadi-Baloutaki, R. Carriveau and D. S. Ting, "Straight-bladed vertical axis wind turbine rotor design guide based on aerodynamic performance and loading analysis", Proc. Inst. Mech. Eng., Part A: J. Power Energy, DOI:10.1177/0957650914538631, Vol. 228, No.7, pp. 742-759, June 9, 2014. (Article)

[29] H. Robert, N. Qin, J. Edwards, and N. Durrani, "Wind tunnel and numerical study of a small vertical axis wind turbine", Renewable energy, DOI:10.1016/j.renene.2009.07.025, Vol. 35, No. 2, pp. 412-422, February 2010. (Article)

[30] Sandia National Laboratory Energy Report, Available at: https://www.osti.gov/servlets/purl/6548367/, accessed January 2023. (Report)

[31] MC Claessens, "The design and testing of airfoils for application in small vertical axis wind turbines," Master Thesis, Delft University of Technology, Delft, Netherlands, 2006. (Book)

[32] M. H. Mohamed, "Performance investigation of H-rotor Darrieus turbine with new airfoil shapes", Energy, DOI:10.1016/j.energy.2012.08.044, Vol.47, No.1, pp.522-530, November 2012. (Article)

[33] Z. Alnasir and M. Kazerani, "Performance comparison of standalone SCIG and PMSG-based wind energy conversion systems" , 27th Canadian Conference on Electrical and Computer Engineering, Toronto, Canada, pp. 1-8. 4-7 May 2014. (Conference Paper)

[34] Orlando, A. Natalia, L. Marco, A. M Rosa and D. Antonio, "A survey of control issues in PMSG-based small wind-turbine systems." IEEE Trans. Ind. Inf., DOI:10.1109/TII.2013.2272888, Vol.9, No.3, pp.1211-1221, July 2013. (Article)

[35] A. Harrouz, I. Colak and K. Kayisli, "Control of a small wind turbine system application", International Conference on Renewable Energy Research and Applications, Birmingham, United Kingdom, pp. 1128-1133, 4-7 May 2014. (Conference Paper)

[36] A. Belkaid, I. Colak, K. Kayisli. and R. Bayindir, "Modeling of a Permanent Magnet Synchronous Generator in a Power Wind Generation System with an Electrochemical Energy Storage", International Journal of Smart Grid-ijSmartGrid, Vol.2, No.4, pp.197-202, December 2018. (Article)

[37] S. Balci and M. Colak, "Performance

Analysis of a Permanent Magnet Synchronous Generator with Parametric Solution Software", 10th International Conference on Smart Grid (icSmartGrid), IEEE. Istambul, Turkey, pp. 443-447, 27-29 June 2022. (Conference Paper)